ACS Macro Letters

Letter

pubs.acs.org/macroletters

Synthesis and Self-Assembly of a Nanoscaled Multiarm Polymer Terminated by β-Cyclodextrin

Jingjing Wang, Jialiang Zhang, Shuling Yu, Wei Wu,* and Xiqun Jiang*

Laboratory of Mesoscopic Chemistry and Department of Polymer Science and Engineering, College of Chemistry and Chemical Engineering, Nanjing University, Nanjing 210093, P. R. China

Supporting Information

ABSTRACT: Giant multiarm polymers with and without β-cyclodextrin (β-CD) end groups were synthesized. Further, the former was assembled into nanoparticles via a β-CD/adamantane inclusion complex. The incorporation of an esterase-sensitive linker in the inclusion complex enables the nanoparticles to decompose to the multiarm polymer again through the hydrolysis of ester linkage, making the nanoparticles have the characteristics of multistage nanovectors.

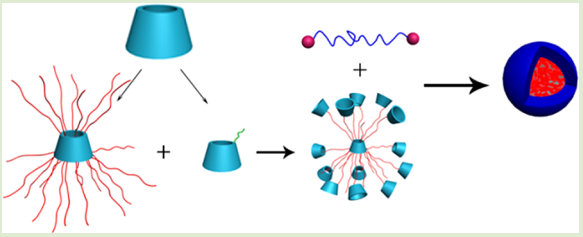

Nano drug delivery systems (NDDSs) can improve the pharmacological profiles of clinical chemtherapeutic agents, making it possible to maximize their therapeutic efficacy while minimizing unwanted side effects, and thus have brought about new hope for cancer treatment.[1] However, it is difficult for one set of NDDSs to efficiently break through all the biological barriers to localize at their targets. To address this dilemma, a strategy of multistage nanovectors (MSVs) was proposed. MSVs are the systems that accommodate two or more sets of nanoelements, each of which is designed to tackle specific biological barriers. Up to now, several examples of MSVs have been reported. As the first example, Tasciotti and co-workers reported a MSV composed by mesoporous silicon particles with functionalized quantum dots (QDs) and single-walled carbon nanotubes (SWNTs) embedded in their pores.[2] The authors envisioned that the MSV had long blood circulation time and thus had a good chance to reach the endothelium where QDs and SWNTs would be released and penetrate into the tissue matrix. Later, Wong and co-workers designed a system of MSVs by covalently linking 10 nm QDs onto the surface of protease-degradable gelatin nanoparticles (100 nm in size). Once the MSVs reached the tumor site, the gelatin nanoparticles could be efficiently degraded by matrix metalloproteinases, and hence QDs would be released and penetrate deep into the tumor matrix due to their small size.[3] Very recently, Fan et al. prepared a type of nanoparticle with diameter of ∼128 nm by dialyzing an amphiphilic oligolysine/iridium (III) complex. In the acidic lysosome environment, the unreacted amino groups in the complex would be more protonated and thus became repulsive to each other, driving the large nanoparticle to dissociate into small ones.[4]

We consider that the assembly of nanoscaled molecules into larger nanoparticles can be an alternative and effective way to prepare MSVs, in which the larger nanoparticles should be designed to be able to decompose into small nanoscaled molecules in the tumor microenvironment and the small vectors can transport drug payloads deep in the tumor.

Herein, we present the synthesis of a giant multiarm polymer terminated by β-cyclodextrin (β-CD) and the assembly of this polymer into nanoparticles via the β-CD/adamantane inclusion complex. Ester linkage is introduced to the nanoparticles by design, which enables the nanoparticles to decompose into the multiarm polymers again by hydrolysis of the ester linkage. Thus, this system has the characteristics of MSVs with the nanoparticle as the first stage vector and the giant multiarm polymer as the second stage vector, which may be very promising in delivering anticancer agents, since the first stage vector can prolong the blood circulation time of anticancer agents thanks to its relatively larger size and the second stage vector can penetrate deep into the tumor matrix due to its smaller size. The multiarm polymer is synthesized by atom transfer radical polymerization (ATRP). Thus, the preparation is facile, and its molecular weight and distribution can be well controlled. The multiarm polymer has abundant hydroxy groups in the peripheral β-CD moieties which can be used to conjugate drug or other bioactive molecules.

As shown in Scheme 1, the synthetic route of the multiarm polymer with β-CD terminal groups includes the synthesis of a β-CD-based polyfunctional ATRP initiator and the successive polymerization of methyl acrylate (MA) and a β-CD-based monomer by ATRP. The β-CD-based polyfunctional ATRP initiator, containing 21 Br groups, named 21-Br-β-CD, was synthesized following published procedures (see Figure S1 in the Supporting Information for ^{1}H NMR of 21-Br-β-CD).[5] The monovinyl β-CD-based monomer, named Triazol-CD-Monomer (Scheme 1), was synthesized by a four-step reaction. Mono-(6-*O*-(*p*-tolylsulfonyl))-β-cyclodextrin was first synthesized following known procedures[6,7] and subsequently reacted with diaminotriethylene glycol, yielding a β-CD derivative with

Received: October 13, 2012
Accepted: December 24, 2012
Published: December 31, 2012

Scheme 1. Schematic Illustration of the Synthesis Routes of the Multiarm Polymer and Self-Assembled Nanoparticles[a]

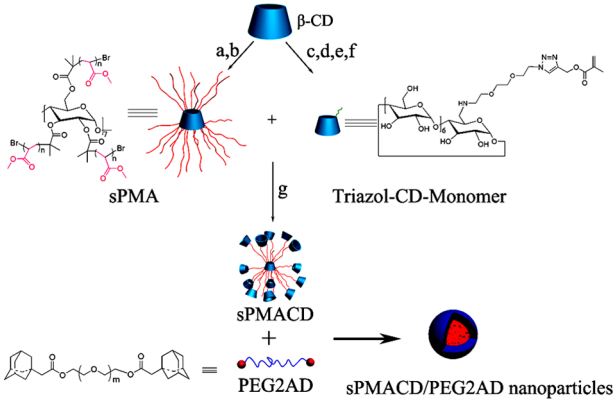

[a](a) 2-Bromoisobutyryl bromide, anhydrous pyridine, anhydrous chloroform, 4-(*N*,*N* dimethylamino) pyridine; (b) Methyl acrylate, PMDETA, CuBr, 70 °C; (c) *p*-TsCl, NaOH; (d) 1,8-Diamino-3,6-dioxaoctane, anhydrous NMP, KI, 70 °C; (e) DMSO/methanol, copper(II) sulfate pentahydrate, potassium carbonate, imidazole-1-sulfonyl azide hydrochloride; (f) 2-propynyl 2-methacrylate, copper-(II) sulfate pentahydrate, sodium ascorbate, H_2O/DMSO, 70 °C; (g) PMDETA, CuBr, 70 °C.

an amino terminus. After transformation of the amino to azide group by using imidazole-1-sulfonyl azide hydrochloride,[8] the "click reaction" of the Huisgen 1,3-dipolar cycloaddition between propargyl methacrylate and the azide group was performed to produce Triazol-CD-Monomer[9] (Scheme 1). The structures of Triazol-CD-Monomer and its precursor compounds were confirmed by electrospray ionization mass spectrometry (ESI-MS) (see Figure S2 in Supporting Information). The diaminotriethylene glycol spacer was introduced to improve the solubility of the monomer and reduce the steric hindrance of polymerization.

The next synthesis step is polymerizing successively the monomer of MA and Triazol-CD-Monomer by using 21-Br-*β*-CD as a core initiator via ATRP to provide the multiarm polymer terminated by *β*-CD (sPMACD, Scheme 1). The detailed procedures are described in the experimental section (see Supporting Information).

Figure 1 shows the comparison of the ^{1}H NMR spectra of sPMACD and sPMA (Scheme 1). In the spectrum of sPMA, the signals located at 3.57, 2.20, and 1.61 ppm can be assigned

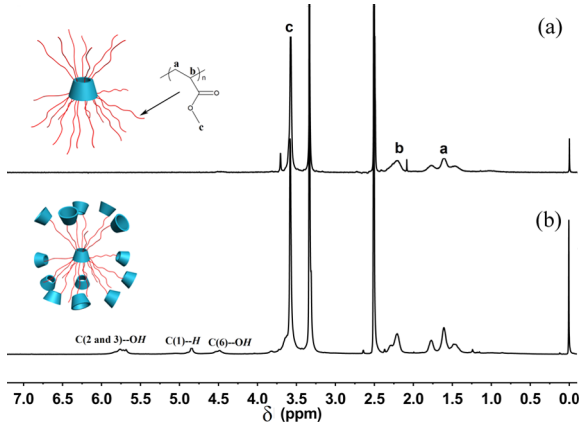

Figure 1. ^{1}H NMR spectra of sPMA (a) and sPMACD (b).

to the protons of $-CH_3$, $-CH-$, and $-CH_2-$ of the poly(methyl acrylate) (PMA) arms, respectively. Due to the low proportion of the CD core, its signals are not observed in the spectrum. In the spectrum of sPMACD, the signals at 5.75, 4.84, and 4.48 ppm can be assigned to the protons of C(2 and 3)−OH, C(1)−H, and C(6)−OH of *β*-CD end groups, respectively. By comparing the integral intensity of the signals at 3.57 and 4.84 ppm, resulting from the $-CH_3$ of the PMA moiety and C(1)−H of the *β*-CD moiety, respectively, the molar ratio of *β*-CD to MA repeating units in sPMACD can be calculated to be 1:27.7 (see Figure S3 in the Supporting Information for the intergral intensity of the proton signals of sPMACD). On the basis of this result, it can be concluded that about 90% of the PMA arm is terminated by one *β*-CD in the second ATRP step. It is worth mentioning that in our experiments we have tried to polymerize more Triazol-CD-Monomers in one arm by using excessive monomers; however, it did not work, which could be caused by the bulky size of the *β*-CD that imparts significant steric hindrance to the polymerization, even if there is a diaminotriethylene glycol spacer between the vinyl group and *β*-CD moiety.

The molecular weight and distribution of sPMA and sPMACD were assessed by gel permeation chromatography (GPC) (Figure 2) and matrix-assisted laser desorption

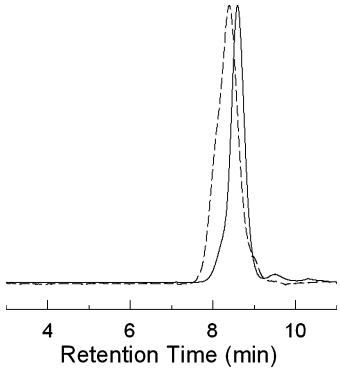

Figure 2. GPC traces of sPMA (solid line) and sPMACD (dashed line).

ionization, time-of-flight mass spectrometry (MALDI-TOF MS) (see Figure S4 in the Supporting Information). On the basis of the GPC measurements, the number-average molecular weight and the polydispersity of sPMA were calculated to be 49687 and 1.10; in contrast, those of sPMACD were 76363 and 1.34, respectively, which are well consistent with the results from MALDI-TOF. On the basis of the difference value between the molecular weight of sPMA and sPMACD, it can be calculated that about 19 *β*-CD molecules are conjugated to one sPMA molecule in the second ATRP step, which is very close to the results of ^{1}H NMR stated above. In addition, the results of GPC also reveal that the intermolecular coupling did not occur during the polymerization since only one peak is observed in the GPC curve of either sPMA or sPMACD.

sPMA and sPMACD were also structurally characterized by Fourier transform infrared spectroscopy (FT-IR) (see Figure S5 in the Supporting Information). In the spectrum of sPMA, an absorption band of the carbonyl stretching vibration can be observed at around 1726 cm^{-1}. Compared to the spectrum of sPMA, the appearance of the absorption bands of the C−O−C stretching vibration at ∼1029 cm^{-1} and the O−H stretching vibration at ∼3352 cm^{-1} in the spectrum of sPMACD suggests

dx.doi.org/10.1021/mz300538u | *ACS Macro Lett.* 2013, 2, 82−85

that β-CD is coupled with sPMA in the second ATRP step, since thorough purification was carried out before the characterization.

The morphological structures of the two types of multiarm polymers of sPMA and sPMACD were investigated by high-resolution transmission electron microscopy (HR-TEM) (Figure 3a and b). It can be seen from the HR-TEM images

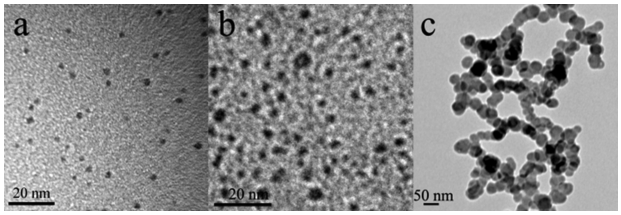

Figure 3. TEM images of sPMA (a), sPMACD (b), and inclusion complexation nanoparticles between sPMACD and PEG2AD (c).

that both of the two types of multiarm polymers have nanoscaled size. The diameter of sPMA is 2.3 ± 0.6 nm with very narrow distribution; in contrast, the molecules of sPMACD have a larger diameter of 3.6 ± 1.0 nm with a relatively broad distribution, which is well consistent with the results of GPC stated above.

It has been well documented that a stable inclusion complex can be formed between β-CD and adamantine in an aqueous medium.[10−13] In light of this, we executed the assembly of sPMACD via the β-CD/adamantane inclusion complex. Adamantyl-modified poly(ethylene glycol) (PEG2AD, Scheme 1) was first synthesized by the esterification between the two terminal hydroxyl groups of poly(ethylene glycol) (PEG, M_n = 1000) and dicyclohexylcarbodiimide (DCC)-activated adamantane acetic acid. The attachment of adamantane acetic acid to the PEG chain is demonstrated by ^{1}H NMR, ^{13}C NMR, and ESI-MS spectra (see Figures S6−S8 in the Supporting Information). To further confirm the complete reaction of the hydroxyl termini of the PEG molecules, a trichloroacetyl isocyanate (TCAI) reagent was mixed with adamantyl-modified PEG since TCAI is well-known to react quantitatively with hydroxyl groups and thereby cause a downfield shift of the α-hydroxymethylene protons.[14,15] Upon the addition of an excess of TCAI to the NMR solutions of adamantane-modified PEG, no such downfield shift was observed, indicating that the terminal hydroxyl groups of the initial PEG have quantitatively reacted with adamantyl groups.

The assembly behavior of the nanoscaled molecule of sPMACD in the presence of adamantyl-terminated PEG was investigated. It is found that when the molar ratio between the β-CD end groups of sPMACD and the adamantine from PEG2AD is 1:1, spherical assemblies (sPMACD/PEG2AD nanoparticles, Scheme 1) are formed with a narrowly distributed diameter of 37.0 ± 5.0 nm (Figure 3c). The assembly mechanism can be explained as follows. In an aqueous medium, the inclusion complex between β-CD and adamantine would be formed, and in this process, two or more sPMACD molecules could be tethered together. Furthermore, in the complexes of sPMACD and PEG2AD, there exist hydrophilic moieties of PEG segments and hydrophobic moieties of PMA segments. Therefore, in the aqueous medium, the assemblies would be formed by exposing the hydrophilic PEG segments to the medium and encapsulating the hydrophobic moieties as the core to minimize the energy of the system.

The cytotoxicity of sPMACD and sPMACD/PEG2AD nanoparticles against the cancer cells, human neuroblastoma SH-SY5Y cells, was investigated. The cell viability was determined after 48 h of incubation with a series of doses of sPMACD and sPMACD/PEG2AD nanoparticles, respectively. For both of the materials, no significant cytotoxicity is observed with a concentration up to 200 μg/mL (see Figure S9a in the Supporting Information), demonstrating the cytocompatibility of sPMACD and sPMACD/PEG2AD nanoparticles. Additionally, after labeling sPMACD and sPMACD/PEG2AD nanoparticles with rhodamine B isothiocyanate (RBITC) via the reaction of the hydroxyl group on the CD moiety with the isothiocyanate group on the dye, we investigated the cellular uptake of the two materials by using laser scanning confocal microscopy (LSCM). Figure S9b in the Supporting Information shows the typical LSCM images of the SH-SY5Y cells coincubated with the two materials at 37 °C for 4 h, respectively. It can be seen that both the sPMACD (red color) and sPMACD/PEG2AD nanoparticles (red color) can be internalized readily by SH-SY5Y cells, which is very important for their applications in drug delivery.

To validate the degradability of the sPMACD/PEG2AD nanoparticles and their potential applications as MSVs, we studied the disassembly behavior of the nanoparticles in the presence of porcine liver esterase (PLE) that are expected to catalyze the hydrolysis of the ester bonds in the nanoparticles.[16] The process of the nanoparticle disassembly was monitored by pyrene fluorescence assay and transmission electron microscopy (TEM), respectively. After encapsulating the pyrene molecules in the hydrophobic region of the nanoparticles, the disassembly of sPMACD/PEG2AD nanoparticles can then be traced by the decrease of the fluorescence of pyrene.[17] From Figure 4, it can be seen that the fluorescence intensity of pyrene

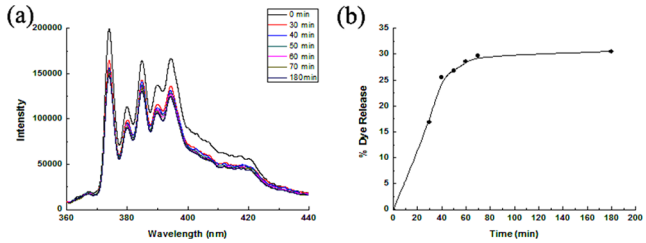

Figure 4. (a) Emission spectra of pyrene encapsulated in sPMACD/PEG2AD nanoparticles after the addition of PLE at different time points. (b) % Release of pyrene from sPMACD/PEG2AD nanoparticles upon exposure to PLE using fluorescence studies.

decreases gradually after exposure to PLE and reaches a plateau at 70% of the initial fluorescence intensity at 3 h after the addition of PLE. Also, the release amount of pyrene from the nanoparticles is 30% in the presence of PLE within the initial 200 min, and then no pyrene release was observed (Figure 4b). To confirm that the decrease of fluorescence intensity and the initial pyrene release are caused by the disassembly of the nanoparticles, we monitored the fluorescence intensity of the pyrene encapsulated by sPMACD/PEG2AD nanoparticles in an aqueous medium in the absence of PLE and found that the fluorescence remained unchanged within 3 h (see Figure S10 in the Supporting Information). These experiments demonstrate that the PLE can effectively catalyze the disassembly of sPMACD/PEG2AD nanoparticles. To understand the appearance of the plateau, we mixed sPMACD and pyrene at the same

dx.doi.org/10.1021/mz300538u | ACS Macro Lett. 2013, 2, 82−85

concentrations as the above system and found that the fluorescence intensity from pyrene is very close to the fluorescence intensity at the plateau, suggesting that the nanoparticles have been decomposed into sPMACD and the plateau is caused by the hydrophobic backbone of the sPMACD and the cavity of the β-CD in the polymer that are capable of solvating a part of pyrene (see Figure S11 in the Supporting Information). The TEM image of the nanoparticles coincubated with PLE for 3 h shows small nanoparticles with the size close to the sPMACD, further demonstrating that the nanoparticles can be decomposed into sPMACD under the catalysis of PLE (see Figure S12 in the Supporting Information). On the basis of these results, it is preliminarily demonstrated that the nanoparticles can be disassemblied from themselves and can accumulate effectively in tumor tissue to small giant multiarm polymers that can diffuse well in the tumor matrix in vivo and thus have the characteristics of MSVs.

In conclusion, a giant multiarm polymer with almost each arm terminated by a β-CD was synthesized by ATRP initiated from a polyfunctional β-CD-based initiator and characterized by NMR, IR, GPC, and TEM. The multiarm polymers, sPMA and sPMACD, had a diameter of 2.3 and 3.6 nm, respectively, and the latter was further assembled into nanoparticles via a β-CD/adamantane inclusion complex with narrowly distributed diameter of 37.0 nm. Both sPMACD and sPMACD/PEG2AD nanoparticles have no obvious cytotoxicity and can enter cells readily. Pyrene fluorescence assay and TEM observation demonstrate that the nanoparticles can be decomposed into small particles under the catalysis of PLE. This type of nanoparticle should be very promising in the applications of drug delivery as multistage nanovectors since there are abundant hydroxyl groups in the β-CD moieties that can be used to conjugate drug or other bioactive molecules, and there are ester linkages between PEG and adamantine moieties that can be hydrolyzed under the catalysis of enzyme in the body. When the nanoparticles enter the circulation system, their relatively larger nanosize would facilitate their accumulation in tumors via the enhanced permeability and retention (EPR) effect. Inside tumor tissues, the ester linkages would be cleaved rapidly under the catalysis of esterase, and the sPMACD would then be released and penetrate deeper into the matrix of the tumor carrying drug payloads.

■ ASSOCIATED CONTENT

Ⓢ Supporting Information

Detailed experimental procedures and additional results. This material is available free of charge via the Internet at http://pubs.acs.org.

■ AUTHOR INFORMATION

Corresponding Author

*E-mail: wuwei@nju.edu.cn; jiangx@nju.edu.cn.

Notes

The authors declare no competing financial interest.

■ ACKNOWLEDGMENTS

This study was supported by the Natural Science Foundation of China (Nos. 51033002 and 51273090) and the Natural Science Foundation of Jiangsu Province (No. BK2010303). Additionally, thanks to Dr. Zhirong Geng from State Key Laboratory of Coordination Chemistry, Nanjing University, for his kind helps in mass spectrometric characterization.

■ REFERENCES

(1) Wang, A. Z.; Langer, R.; Farokhzad, O. C. *Annu. Rev. Med.* **2012**, *63*, 185−198.
(2) Tasciotti, E.; Liu, X.; Bhavane, R.; Plant, K.; Leonard, A. D.; Price, B. K.; Cheng, M.; Decuzzi, P.; Tour, J. M.; Robertson, F.; Ferrari, M. *Nat. Nanotechnol.* **2008**, *3*, 151−157.
(3) Wong, C.; Stylianopoulos, T.; Cui, J.; Martin, J.; Chauhan, V. P.; Jiang, W.; Popovic, Z.; Jain, R. K.; Bawendi, M. G.; Fukumura, D. *Proc. Natl. Acad. Sci. U.S.A.* **2011**, *108*, 2426−2431.
(4) Fan, Y.; Li, C.; Cao, H.; Li, F.; Chen, D. *Biomaterials* **2012**, *33*, 4220−4228.
(5) Plamper, F. A.; Becker, H.; Lanzendörfer, M.; Patel, M.; Wittemann, A.; Ballauff, M.; Müller, A. H. E. *Macromol. Chem. Phys.* **2005**, *206*, 1813−1825.
(6) Amajjahe, S.; Choi, S.; Munteanu, M.; Ritter, H. *Angew. Chem., Int. Ed.* **2008**, *47*, 3435−3437.
(7) Law, H.; Benito, J. M.; García Fernández, J. M.; Jicsinszky, L.; Crouzy, S.; Defaye, J. *J. Phys. Chem. B* **2011**, *115*, 7524−7532.
(8) Goddard-Borger, E. D.; Stick, R. V. *Org. Lett.* **2007**, *9*, 3797−3800.
(9) Amajjahe, S.; Munteanu, M.; Ritter, H. *Macromol. Rapid Commun.* **2009**, *30*, 904−908.
(10) Burckbuchler, V.; Wintgens, V.; Lecomte, S.; Percot, A.; Leborgne, C.; Danos, O.; Kichler, A.; Amiel, C. *Biopolymers* **2006**, *81*, 360−370.
(11) Bartlett, D. W.; Davis, M. E. *Bioconjugate Chem.* **2007**, *18*, 456−468.
(12) Ge, Z. S.; Liu, H.; Zhang, Y. F.; Liu, S. Y. *Macromol. Rapid Commun.* **2011**, *50*, 7407−7409.
(13) Böhm, I.; Isenbügel, K.; Ritter, H.; Branscheid, R.; Kolb, U. *Angew. Chem., Int. Ed.* **2011**, *123*, 7545−7547.
(14) Postma, A.; Davis, T. P.; Donovan, A. R.; Li, G. X.; Moad, G.; Mulder, R.; O' Shea, M. S. *Polymer* **2006**, *47*, 1899−1911.
(15) Donovan, A. R.; Moad, G. *Polymer* **2005**, *46*, 5005−5011.
(16) Patel, K.; Angelos, S.; Dichtel, W. R.; Coskun, A.; Yang, Y. W.; Zink, J. I.; Stoddart, J. F. *J. Am. Chem. Soc.* **2008**, *130*, 2382−2383.
(17) Azagarsamy, M. A.; Sokkalingam, P.; Thayumanavan, S. *J. Am. Chem. Soc.* **2009**, *131*, 14184−14185.